Light scattering, electrophoresis, and turbidimetry studies of bovine serum albumin-poly(dimethyldiallylammonium chloride) complex

Jiulin Xia, Paul L. Dubin, and Herbert Dautzenberg

Langmuir, **1993**, 9 (8), 2015-2019 • DOI: 10.1021/la00032a020

Light Scattering, Electrophoresis, and Turbidimetry Studies of Bovine Serum Albumin–Poly(dimethyldiallylammonium chloride) Complex

Jiulin Xia,† Paul L. Dubin,*,† and Herbert Dautzenberg‡

Department of Chemistry, Indiana University—Purdue University at Indianapolis, Indianapolis, Indiana 46205, and Max Planck Institute for Colloid and Interface Research, Teltow-Seehof O-1530, Germany

Received December 21, 1992. In Final Form: May 13, 1993

Complexation between bovine serum albumin (BSA) and poly(dimethyldiallylammonium chloride) (PDMDAAC) was studied by static and quasi-elastic light scattering (QELS), electrophoretic light scattering, and turbidimetric titration in dilute electrolyte solution. Both QELS and turbidimetric titration show that complexation occurs at pH > 4.6. The structure of the BSA–PDMDAAC complex in excess protein solution at ionic strength 0.01 M and pH 7.88 depends on the polymer concentration. At low polymer concentration, an intrapolymer complex saturated with BSA is formed. This intrapolymer complex aggregates to interpolymer species upon increase in the polymer concentration.

Introduction

Protein–polyelectrolyte complexes (PPCs) can play an important role in a variety of chemical and biological processes, such as protein separation,[1-3] enzyme stabilization,[4,5] and polymer drug delivery.[6,7] Also, by studying PPC formation we may improve our understanding of interactions between proteins and nucleic acid in the transcription process.[8] The nature of the polyelectrolytes and proteins comprising the complexes controls their chemical and biological properties, as well as their composition, structure, and size. Therefore, molecular weight (MW) and size measurements of PPCs are particularly important since both composition and structure can be deduced from these measurements. However, MW measurement is difficult. The concentration dependence of PPC structure obstructs the classical analysis of light scattering data by, e.g., Zimm plots. The same effect interferes with size exclusion gel permeation chromatography because the sample under study undergoes substantial dilution during the measurement process, leading to PPC dissociation or structure change.

Recently, Dautzenberg et al.[9] reported on the static light scattering of complexes formed from the enzyme invertase and a polycation. A similar study on antigen–antibody complex was carried out by Yarmush et al.[10] These measurements are successful due to the following reason: all the complexes were studied under conditions of excess protein so that the solution contains only complex and free protein. Since the scattering intensity from the former is dominant in such a system, light scattering may be used to characterize the complex.

We have recently used various techniques to study protein–polyelectrolyte complexation as a function of pH, ionic strength, and polymer concentration.[11-14] Depending on these variables, complexes can be formed as soluble, colloidal, or precipitated species. In this paper, we concentrate on the elucidation of the molecular structure of stable equilibrium complexes of BSA–PDMDAAC by static light scattering, photon correlation spectroscopy, and electrophoretic light scattering. The details of the structure and the exact conditions under which various complex states are stable will differ from one polyelectrolyte–protein pair to another; however, the instrumental methodologies and the general approaches to interpretation of the data presented herein are expected to serve as guidelines in studies of other protein–polyelectrolyte systems.

Experimental Section

Materials. Poly(dimethyldiallylammonium chloride) (PDMDAAC), a commercial sample of Merquat 100 from Calgon Corporation (Pittsburgh, PA) with a nominal molecular weight (MW) of 2×10^5 and reported polydispersity of $M_w/M_n \geq 10$,[15] was dialyzed (12000–14000 nominal MW cut-off) and freeze-dried before use. From light scattering on the freeze-dried material we obtain $M_w = 2.0 \times 10^5$. Bovine serum albumin (BSA) with $M_w = 6.7 \times 10^4$, was obtained from Sigma Chemical as 95–99% pure and used as received. All water was deionized and distilled.

Methods. *Turbidimetry.* Turbidity measurements were made at 420 nm with a Brinkmann PC800 probe colorimeter, equipped with a 2.0 cm path length fiber optics probe. Type 1 titrations were carried out at 24 °C by addition of 0.1 M NaOH, with a micrometer buret, to a solution of 0.5 g/L BSA in 0.01 M NaCl, at varying BSA/PDMDAAC (w/w) ratio (r), and recording $100 - \%\ T$. A protein blank correction was made under the same conditions in the absence of the polymer.

† Indiana University—Purdue University at Indianapolis.

‡ Max Planck Institute for Colloid and Interface Research.

(1) Bozzano, A. G.; Andrea, G.; Glatz, C. E. *J. Membr. Sci.* **1991**, *55*, 181.
(2) Clark, K. M.; Glatz, C. E. *Biotechnol. Prog.* **1987**, *3*, 241.
(3) Fisher, R. R.; Glatz, C. E. *Biotechnol. Bioeng.* **1988**, *32*, 777.
(4) Margolin, A.; Sheratyuk, S. F.; Izumrudov, V. A.; Zezin, A. B.; Kabanov, V. A. *Eur. J. Biochem.* **1985**, *146*, 625.
(5) Ruckpoul, K.; Rein, H.; Janig, G. R.; Pfeil, W.; Ristau, O.; Damaschun, B.; Damaschun, H.; Muller, J. J.; Purschel, H. V.; Bleke, J.; Scheler, W. *Stud. Biophys.* **1972**, *34*, 81.
(6) Regelson, W. *Interferon* **1970**, *6*, 353.
(7) Ottenbrite, R. M.; Kaplan, A. M. *Ann. N. Y. Acad. Sci.* **1985**, *446*, 160.
(8) Shaner, S. L.; Melancon, P.; Lee, K. S.; Burgess, R. R.; Record, M. T., Jr. *Cold Spring Harbor Symp. Quant. Biol.* **1983**, *47*, 463.
(9) Dautzenberg, H.; Rother, G. *J. Appl. Polym. Sci.: Appl. Polym. Symp.* **1991**, *48*, 351.
(10) Murphy, R. M.; Slayter, H.; Schurtenberger, P.; Chamberlin, R. A.; Colton, C. K.; Yarmush, M. L. *Biophys. J.* **1988**, *54*, 45.
(11) Park, J. M.; Muhoberac, B. B.; Dubin, P. L.; Xia, J. *Macromolecules* **1992**, *25*, 290.
(12) Strege, M. A.; Dubin, P. L.; West, J. S.; Daniel Flinta, C. D. In *Protein Purification: from Molecular Mechanisms to Large-Scale Processes*; Ladisch, M., Willson, R. C., Painton, C. C., Builder, S. E., Eds.; American Chemical Society: Washington, DC, 1990; Chapter 5.
(13) Dubin, P. L.; Murrell, J. M. *Macromolecules* **1988**, *21*, 2291.
(14) Dubin, P. L.; Ahmed, L.; Xia, J. Submitted for publication.
(15) Lin, F. M., Calgon Corp., private communication.

0743-7463/93/2409-2015$04.00/0

Sample Preparation. All solutions were prepared by mixing dust-free (filtered by Gelman 0.2 μm syringe filters) stock solutions of the individual components. The concentration of BSA was 0.5 g/L, and pH was kept at 7.88 in 0.01 M phosphate buffer. Solutions for type 1 titration were prepared in 0.01 M NaCl instead of phosphate buffer in order to maintain constant ionic strength.

Quasi-Elastic Light Scattering (QELS). QELS measurements were made at scattering angles from 30° to 150° with a Brookhaven (Holtsville, NY) 72-channel BI-2030 AT digital correlator and using a Jodon 15-mW He–Ne laser (Ann Arbor, MI). A 200-μm pinhole aperture was used for the EMI photomultiplier tube, and decahydronaphthalene (decalin) was used as the refractive index matching fluid to reduce stray light. We obtain the homodyne intensity–intensity correlation function $G(q,t)$, with q, the amplitude of the scattering vector, given by $q = (4\pi n/\lambda)\sin(\theta/2)$, where n is the refractive index of the medium, λ is the wavelength of the excitation light in a vacuum, and θ is the scattering angle. For a Gaussian distribution of intensity profile of the scattered light, $G(q,t)$ is related to the electric field correlation function $g(q,t)$ by

$$G(q,t) = A(1 + bg(q,t)^2) \tag{1}$$

where A is the experimental baseline and b is a constant, which depends on the number of coherence areas that generates the signal ($0 < b < 1$). The quality of the measurements was verified by determining that the difference between the measured value of A and the calculated one was less than 1%. The electric field correlation function depends on the Fourier transform of the fluctuating number density of particles or molecules. For the center of mass diffusion of identical particles, the following simple relation holds

$$g(q,t) = e^{-t/\tau}$$

$$1/\tau = Dq^2 \tag{2}$$

where τ is decay time and D is diffusion coefficient. More detailed discussions of QELS data analysis may be found in refs 16 and 17.

For polydisperse systems the correlation function $g(q,t)$ can be expressed as an integral of the exponential decays weighted over the distribution of relaxation times $\rho(\tau)$

$$g(t) = \int_0^\infty e^{-t/\tau}\rho(\tau)\,d\tau \tag{3}$$

In principle, it is possible to obtain the distribution $\rho(\tau)$ by integral transformation of the experimental $[G(t)/A - 1]^{1/2}$, but in practice this presents a formidable problem for numerical analysis, since taking the inverse Laplace transform is numerically an ill-posed problem. Several numerical methods developed so far are devoted to calculating $\rho(\tau)$. In the present work, we analyze the autocorrelation functions by using the CONTIN program, which employs the constrained regularization method.[18]

From eq 3, the mean relaxation time, $\langle\tau\rangle$, defined as the area of $g(t)$, is given by

$$\langle\tau\rangle = \int_0^\infty g(t)\,dt = \int_0^\infty \tau\rho(\tau)\,d\tau \Big/ \int_0^\infty \rho(\tau)\,d\tau \tag{4}$$

This $\langle\tau\rangle$ value can be resolved from each of the distribution modes of $\rho(\tau)$, as the first moment of the normalized relaxation spectrum. Therefore, the diffusion coefficient, which corresponds to each value of $\langle\tau\rangle$, can be calculated using

$$D = \frac{\lambda^2}{16\pi^2 \sin^2(\theta/2)\langle\tau\rangle} \tag{5}$$

From each D value we obtain Stokes' radius, R_s, by the Einstein equation

$$R_s = \frac{kT}{6\pi\eta D} \tag{6}$$

where k is Boltzmann's constant, T is the absolute temperature, and η is the viscosity of the solvent.

Static Light Scattering (SLS). SLS measurements were made with the same Brookhaven system described above. Intensity measurements were calibrated by pure (>99.5%) toluene and optical alignment was ensured by less than 3% deviation from linearity in the $I \sin\theta$ vs θ plot. Each measurement was carried out for 5 s. The average of 10 such measurements was reported as I_s. These values were used to calculate Rayleigh ratio, R_θ. In this R_θ measurement we use as the reference solvent pure BSA solution with the same ionic strength and pH as complex-containing solution.

For PDMDAAC, we used the refractive index increment, $dn/dc = 0.186$, determined by Burkhardt[19] with a differential refractometer. Attempts to measure dn/dc of the complex failed because of scattering effects. Since the complex is comprised of polymer and protein, we calculated $(dn/dc)_x$ of the complex by using

$$\left(\frac{dn}{dc}\right)_x = \frac{1}{1+\beta}\left(\frac{dn}{dc}\right)_p + \frac{\beta}{1+\beta}\left(\frac{dn}{dc}\right)_{pr} \tag{7}$$

where the subscripts x, p, and pr represent complex, polymer, and protein, respectively. β represents the mass ratio of bound protein to polymer, and $(dn/dc)_{pr} = 0.185$ for BSA.[20]

To determine the molecular parameters of a macromolecule, static light scattering results are usually plotted as Zimm diagrams corresponding to the equation

$$\frac{Kc}{R_\theta} = \frac{1}{M_w}\left(1 + \frac{16\pi^2}{3\lambda^2}R_g^2 \sin^2\frac{\theta}{2}\right) + 2A_2c \tag{8}$$

where c is the mass concentration of polymer, K is a constant which contains the optical parameters of the system, M_w and R_g are the weight average molecular weight and the root mean square radius of gyration of the macromolecule, respective, and A_2 is the second virial coefficient.

Electrophoretic Light Scattering (ELS). ELS measurements were made at four scattering angles (8.6°, 17.1°, 25.6°, and 34.2°), using a Coulter (Hialeah, FL) DELSA 440 apparatus. The electric field was applied at a constant current of 5 mA.

In ELS, the photon-counting heterodyne correlation function for a solution with an electrophoretically monodisperse solute can be written as[21]

$$C(\tau) = \beta_0\delta(\tau) + \alpha_0 + \alpha_1 \exp(-2Dq^2\tau) + \alpha_2 \exp(-Dq^2\tau)\cos(\Delta\omega\tau) \tag{9}$$

where β_0, α_0, α_1 and α_2 are constants independent of correlation time, τ, and $\delta(\tau)$ is the delta function. D and q have the same definitions as in QELS. The cosine term is due to simultaneous electrophoresis and diffusion.

The Fourier transform of eq 9 with respect to time, as stipulated by the Weiner–Khinchine theorem,[22] gives the power spectrum

(16) Pecora, R.; Berne, B. J. *Dynamic Light Scattering*; Wiley: New York, 1976.
(17) Stock R. S.; Ray, W. H. *J. Polym. Sci., Polym. Phys. Ed.* **1985**, *23*, 1393.
(18) Provencher, S. W. *Comput. Phys. Commun.* **1982**, *27*, 229.
(19) Burkhardt, C. W.; McCarthy, K. J.; Parazak, D. P. *J. Polym. Sci., Polym. Lett.* **1987**, *25*, 209.
(20) Doty, P. *Adv. Protein Chem.* **1951**, *6*, 35.
(21) Ware, B. R.; Haas, D. D. In *Fast Methods in Physical Biochemistry and Cell Biology*; Shaafi, R. I., Fernandez, S. M., Eds.; Elsevier: Amsterdam, 1983.
(22) McQuarrie, D. A. *Statistical Mechanics*; Harper and Row: New York, 1976; p 553.
(23) Dubin, P.; Hua, J. Unpublished results.

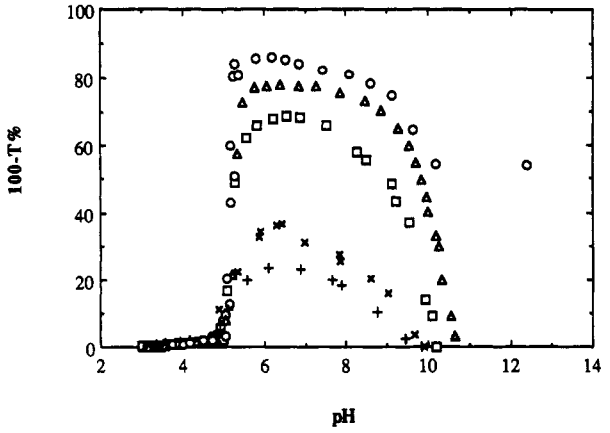

Figure 1. Type 1 titrations of various PDMDAAC concentration in 0.60 g/L BSA and 0.01 M NaCl: r (=0.60/C_p) 10 (○); 50 (△); 100 (□); 300 (×); 500 (+).

$$S(\omega) = \beta_0 + \alpha\delta(\omega) + \frac{2(\alpha_1/\pi)Dq^2}{\omega^2 + (2Dq^2)^2} + \frac{\alpha_2 Dq^2}{2\pi}\left[\frac{1}{(\omega + \Delta\omega)^2 + (Dq^2)^2} + \frac{1}{(\omega - \Delta\omega)^2 + (Dq^2)^2}\right] \quad (10)$$

where α is a constant independent of ω.

In both eqs 9 and 10, $\Delta\omega$ is the difference between the angular frequency of the scattered light, ω_s, and that of the reference beam, ω_r, which is the same as that of the incident beam. Since the frequency of the incident beam is modulated in the scattered light by the amount of the so-called Doppler shift frequency, $\Delta\omega$ is given by

$$\Delta\omega = \frac{2\pi n}{\lambda} Eu \sin\theta \quad (11)$$

where E (V/cm) and u ((μm s^{-1})/(V cm^{-1})) are the applied electric field strength and electrophoretic mobility, respectively. Therefore, u can be directly evaluated from frequencies of the power spectrum. Detailed discussion on ELS measurements can been found in refs 16 and 21.

Results and Discussion

1. BSA–PDMDAAC Complexation at Varying pH and Mass Ratio. Figure 1 shows the type 1 turbidimetric titrations curves of PDMDAAC at various concentrations in 0.60 g/L BSA solution, at ionic strength (I) of 0.01 M NaCl. All of the curves display an abrupt increase in turbidity at pH 5.1, about 0.2 pH unit above the isoelectric point of BSA, corresponding to colloidal complex formation. Prior to colloid formation, we observe a ~2% turbidity increase at pH 4.6 for all polymer concentrations. This small turbidity increase is due to the initial formation of the soluble complex: particles with a size larger than either BSA or PDMDAAC are detected at this pH by QELS, as shown in Figure 2. All solutions exhibit turbidity maxima at *ca.* pH 6.4. These turbidity maxima can be understood from the simultaneous effects of increasing complex size and solubility. It is well-known that protein–polyelectrolyte complexation is a result of electrostatic interactions.[11-14] Therefore, increasing the negative net charge of BSA via increase in pH will enhance its binding to polymer, leading initially to a loss of solubility. After the polymer is saturated with bound BSA, the solubility of the complex may increase with pH because the whole polymer chain is covered by the highly charged proteins. The competition of these size and solubility effects causes the maxima in turbidity.

Figure 2 shows the diameters obtained by QELS for the BSA–PDMDAAC complex as a function of pH for complexes formed at r = 10 and 300, respectively. Clearly, size increases with pH after initial binding in both cases. However, the complex at r = 300 shows a constant diameter of *ca.* 270 nm at pH > 5.80, while the solution at lower r becomes too turbid to measure. The limited size of the complex in the presence of excess protein supports the hypothesis advanced above that the saturated complex may resist higher aggregation.

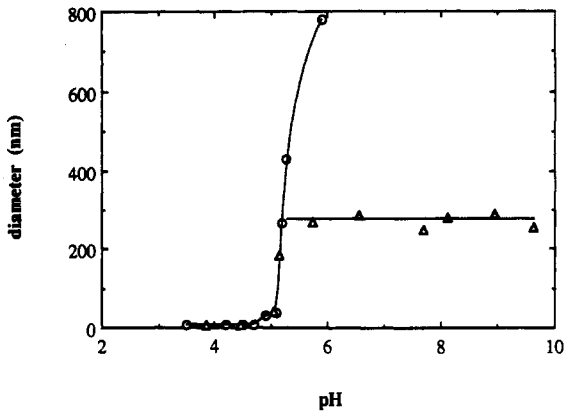

Figure 2. Complex size obtained by QELS as a function of pH for PDMDAAC in 0.60 g/L BSA and 0.01 M NaCl with r (=0.60/C_p) = 10 (○) and 300 (△).

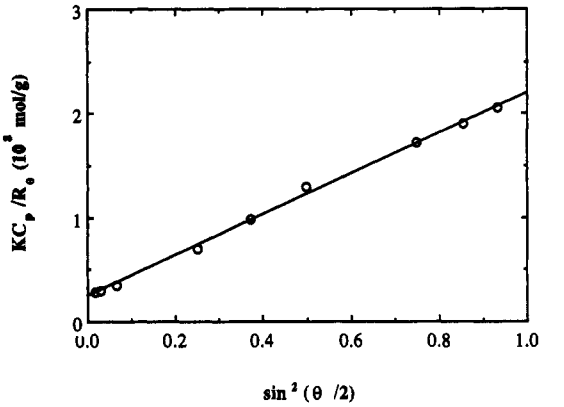

Figure 3. K_c/R_θ vs $\sin^2(\theta/2)$ plot obtained for BSA–PDMDAAC complex with r = 300 in C_{BSA} = 0.60 g/L and 0.01 M phosphate buffer solution of pH 7.88.

2. Static Light Scattering of BSA–PDMDAAC Complex. Prior to static light scattering, the degree of complexation was first estimated by the following procedure. An equilibrium solution at pH 7.88 and ionic strength 0.01, with r = 300 of BSA and PDMDAAC was centrifuged and filtered through a 20-nm filter. The solution obtained was found to be complex-free by QELS. The concentration of free BSA in the solution was then determined by optical density measurement at 280 nm using the reported extinction coefficient of 4.36×10^4.[24] From the free BSA concentration, we obtained $\beta = C_{BSA}/C_p$ = 39, which corresponds to 120 BSA bound per PDMDAAC chain.

Static light scattering results obtained for the complex with r = 300 in 0.01 M phosphate buffer at pH 7.88 are shown in Figure 3. The refractive index increment of the complex was calculated from eq 7 with β = 40. To analyze the SLS results, we ignore the particle interaction term, i.e. the second virial coefficient in eq 8. The error caused by this approximation is less than 5%[10] because of the

(24) Gerald, D. F. In *Practical Handbook of Biochemistry and Molecular Biology*; CRC: Boca Raton, FL, 1989.

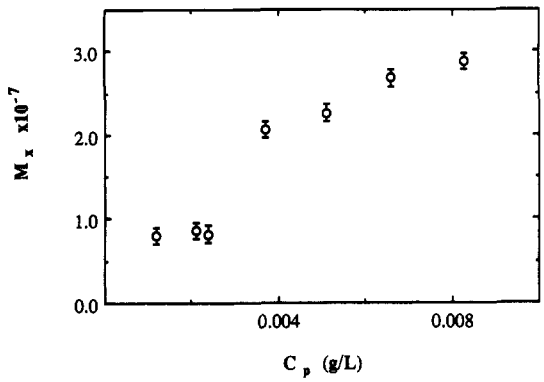

Figure 4. log M_x vs C_p for BSA–PDMDAAC complex in 0.01 M pH 7.88 phosphate buffer with C_{BSA} = 0.60 g/L.

Table I. Hydrodynamic Radius and Radius of Gyration of the BSA–PDMDAAC Complex[a]

C_p (g/L)	R_h (nm)	R_g (nm)	ρ (=R_g/R_h)
1.2×10^{-3}	110	250	2.3
2.1×10^{-3}	115	230	2.0
2.4×10^{-3}	95	240	2.5
3.7×10^{-3}	90	245	2.7
5.1×10^{-3}	110	235	2.2
6.6×10^{-3}	120	290	2.4
8.3×10^{-3}	110	420	3.8

[a] Protein concentration 0.60 g/L, pH = 7.88, ionic strength 0.01 M.

very low polymer concentration. Therefore, eq 8 can be simplified to

$$\frac{Kc_x}{R_\theta} \cong \frac{1}{M_x}\left(1 + \frac{16\pi^2}{3\lambda^2} R_g^2 \sin^2\frac{\theta}{2}\right) \quad (12)$$

where c_x and M_x are the concentration and molecular weight of the complex, respectively. c_x and M_x are related to the polymer concentration and polymer molecular weight by

$$c_x = c_p(1 + \beta) \quad (13)$$

$$M_x = \alpha M_p(1 + \beta) \quad (14)$$

where α is the degree of aggregation, i.e. number of polymer chains within one complex. Substitution of eqs 13 and 14 into eq 12 yields

$$\frac{KC_p}{R_\theta} \cong \frac{1}{\alpha M_p(1 + \beta)^2}\left(1 + \frac{16\pi^2}{3\lambda^2} R_g^2 \sin^2\frac{\theta}{2}\right) \quad (15)$$

Therefore, we may use the known polymer concentration C_p to evaluate the molecular weight of the complex by plotting the angular dependence of the scattered intensity as KC_p/R_θ vs $\sin^2(\theta/2)$ as shown in Figure 3. Such results are plotted in Figure 4 as M_x vs C_p. The constant molecular weight at low polymer concentration of $M_x = 8.1 \times 10^6$ corresponds to a β value of 40 ± 2, which is consistent with the value obtained by filtration. This initially constant β also supports the proposed intrapolymer complex structure.

The radius of gyration of the complex may be obtained from the slope of Figure 3. For different amounts of added polymer, values of R_g and corresponding hydrodynamic radii, obtained from QELS, as well as $\rho = R_g/R_H$, are given in Table I. Hydrodynamic theory[25] shows that ρ changes from infinity to 0.775 when the polymer structure changes from a long rod to a sphere. For a random coil structure,

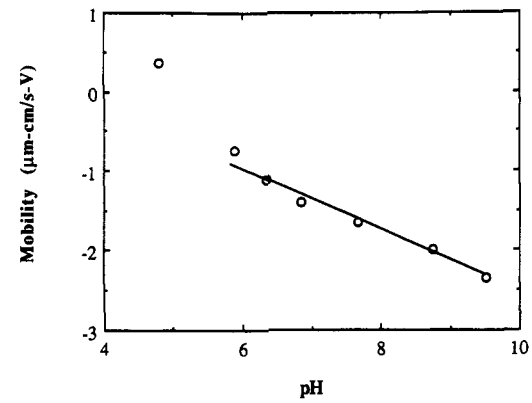

Figure 5. Mobility of BSA–PDMDAAC complex as a function of pH: C_p = 0.002 g/L; C_{BSA} = 0.60 g/L (r = 300); I = 0.01 M NaCl.

ρ assumes values from 1.3 to 1.5.[25] In a previous study,[26] we found through a similar analysis that the complex formed from PEO and SDS micelles behaves like a random coil polymer, and similar results were obtained for the complex of ribonuclease A and sodium polystyrenesulfonate.[27] However, the values for ρ in Table I are intermediate between those of random coil and long rod. The apparent extended structure of these BSA–PDMDAAC complexes could be the result of the interprotein repulsive forces which prevail at low ionic strength and pH well above pI.

3. Electrophoretic Light Scattering of BSA–PDMDAAC Complex. Figure 5 shows the electrophoretic mobility of the complex formed at r = 300 in 0.01 M NaCl as function of pH. The increase in the absolute magnitude of the mobility is due to the simultaneous increase in BSA negative net charge and the number of BSA bound per polymer chain. One may note that the mobility changes sign between pH 4.8 and 5.9. This suggests that the complex initially formed in 4.8 < pH < 5.9 is not saturated by BSA.

Upon further increase in pH above 5.9, the mobility changes linearly with pH. As discussed below, this may be explained on the basis of an intrapolymer complex saturated with BSA. The presence of such species in this pH range is supported by the observation from QELS of constant diameter above pH 5.8. To a first approximation, the mobility of the intrapolymer complex, u, can be written as

$$u = \frac{q_p + nq_{pro}}{f_p + nf_{pro}} = \frac{q_p + nq_{pro}}{f_x} \quad (16)$$

where q_p and q_{pro} are the charges of polymer and protein, respectively, n is the number of proteins bound per polymer chain, and f_p, f_{pro}, and f_x are friction coefficients of polymer, protein, and complex, respectively. This simplified equation treats the behavior of the complex as that of a free-draining "copolymer" with additive contributions from bound proteins and free sequences. Published pH titration curves[28] show that the net charge of BSA (q_{pro}) varies linearly with pH in the range of 6 to 10

$$q_{pro} \cong 26.4 - 6.0\text{pH} \quad (17)$$

From eqs 16 and 17 the mobility is expected to be linear with pH at 6 < pH < 10, as observed, if the friction coefficient of complex f_x is independent of pH. This result is consistent with a saturated state of the complex (i.e. n

(25) Konishi, T.; Yoshizaki, T.; Yamakawa, H. *Macromolecules* **1991**, *24*, 5614.

(26) Xia, J.; Dubin, P.; Kim, Y. S. *J. Phys. Chem.* **1992**, *96*, 6805.
(27) Xia, J.; Dubin, P. Unpublished results.
(28) Tanford, C. *J. Am. Chem. Soc.* **1950**, *72*, 441.

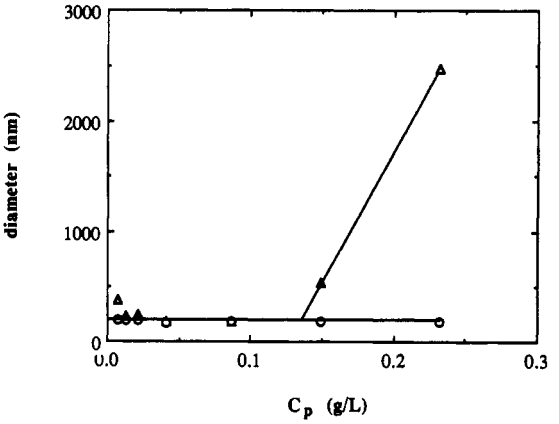

Figure 6. Diameter of BSA–PDMDAAC complex as a function of polymer concentration in 0.60 g/L BSA and 0.01 M phosphate buffer solution with pH 7.88. (O) represents the data obtained for supernatant solution; Δ is from the direct measurements of the complex solution.

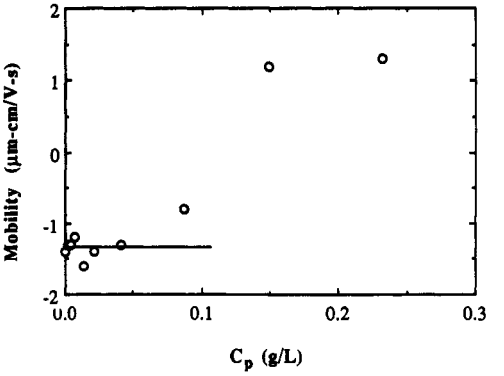

Figure 7. Mobility of BSA–PDMDAAC complex as a function of the polymer concentration in 0.60 g/L BSA and 0.01 M phosphate buffer solution with pH 7.88.

is constant). Substituting eq 17 and $n = 120$ obtained by SLS into eq 16, we obtain $f_x = 3.2 \times 10^{-5}$ P cm, which is much larger than that obtained by the Einstein equation: $f = 6\pi\eta R \approx 2.4 \times 10^{-6}$ P cm. The unrealistic value obtained for f_x may arise from several sources. First, the Einstein relationship is not expected to hold in the present case because of hydrodynamic and electrostatic interactions. A second weakness in the preceding analysis is the neglect of counterion condensation. Nevertheless, the approach embodied in eq 16–17 accounts in the simplest way for observed linear dependence of u on pH.

4. Size and Mobility of BSA–PDMDAAC Primary Intrapolymer Complex. Figure 6 shows the diameter of the BSA–PDMDAAC complex formed in 0.01 M pH 7.88 phosphate buffer and BSA concentration of 0.6 g/L as a function of the polymer concentration, C_p. The triangles represent data obtained by QELS directly on the solution. The circles are from measurements on the supernatant of the solution after 20 min of centrifugation at 10 000 rpm. Up to a polymer concentration of $C_p = 0.13$ g/L, the species formed consistently exhibits a diameter of 190 nm, which is identical to the value obtained from all supernatants. The same value of C_p corresponds to the onset of a plateau in the electrophoretic mobility, as shown in Figure 7. Below this concentration, the mobility exhibits a sign change after displaying a constant value of $u = -1.4$ (μm cm)/(V s) in the range $0 < C_p < 0.05$ g/L. These observations suggest the presence of a primary (intrapolymer) complex at low C_p. Under these conditions, the large excess of protein, along with the strong intrinsic binding that is a consequence of the large negative protein charge (−21 by titration) and low ionic strength, ensures the saturation of each polymer chain. There is essentially no free polymer in these systems at low C_p, only intrapolymer complex and free protein. We estimate that each polymer may bind on the order of 120 protein molecules, corresponding to a net protein charge in excess of −2000. Consequently, the primary complex has a net negative charge and hence a negative mobility, i.e. −1.4 (μm cm)/(V s), as shown in Figure 7. Intrapolymer repulsion among the bound protein molecules causes the chain to expand, with a hydrodynamic radius approximately 4 times larger than the value of the protein-free polymer (R_h = 24 nm). The net negative charge of this complex precludes higher-order association. After sufficient polymer has been added to bind all the free protein, further addition of the polycation leads to flocculation of the primary complexes. Since more than one polymer chain is involved in the flocculation, very large particles of interpolymer complex are observed, as shown in Figure 6 at $C_p > 0.15$ g/L. From electrophoretic light scattering, as shown in Figure 7, we also find the mobility of the complex changing to positive, consistent with multipolymer complex formation. Figure 6 also shows the size obtained for particles after centrifugation. The fact that particle size in the supernatant is the same as the size of the "primary" intrapolymer complex at low C_p suggests that the primary complex is in equilibrium with the separated phase.

Conclusions

The structure of the BSA–PDMDAAC complex in solutions of $C_{pr} = 0.6$, $I = 0.01$ M, and pH 7.88 depends on the polymer concentration. At low polymer concentration, an intrapolymer complex is saturated with BSA. The mass ratio of the bound BSA to polymer in the saturation limit is about 40. This intrapolymer complex aggregates to interpolymer species upon increase in the polymer concentration. The successful application of static light scattering to a complex with unknown concentration could make this technique useful for a variety of systems, including antigen–antibody complexes used in clinical diagnostics.

Acknowledgment. This research was supported by grants from the National Science Foundation (DMR 9014945), American Chemical Society (ACS-PRF#25532-AC7B), Eli Lilly Company, Reilly Industries, and the Exxon Education Fund.